Journal of Materials Chemistry A

Accepted Manuscript

ROYAL SOCIETY OF CHEMISTRY

www.rsc.org/materialsA

J. Mater. Chem. A

COMMUNICATION

Improved electrochemical performance of $Na_{0.67}MnO_2$ through Ni and Mg substitution

Received 00th January 20xx,
Accepted 00th January 20xx

DOI: 10.1039/x0xx00000x

www.rsc.org/

K. Hemalatha,[ab‡] M. Jayakumar,[a‡] Parthasarathi Bera[c] and A. S. Prakash[a]*

Incorporating nickel and magnesium in P2-$Na_{0.67}MnO_2$ is expected to suppress Jahn-Teller active Mn^{3+} ions, increase the average potential of the electrode through Ni^{4+}/Ni^{2+} redox couples and stabilize M–O layers resulting in smooth cycling profile with better capacity retention. In this communication, P2-$Na_{0.67}Ni_{0.25}Mg_{0.1}Mn_{0.65}O_2$ is reported as cathode material for rechargeable Na-ion batteries. It reversibly intercalates ~0.52 moles of Na per formula unit in the voltage region of 1.5 – 4.2 V at C/10 rate which corresponds to a specific capacity of 140 mAh/g. X-ray photoelectron spectroscopy has attributed the origin of the capacity in this phase to both Ni and Mn redox species active at different potential ranges. Substituting part of Mn with Ni and Mg increases the average potential of $Na_{0.67}MnO_2$ and improves the energy density of $Na_{0.67}Ni_{0.25}Mg_{0.1}Mn_{0.65}O_2$ to 335 Wh/kg.

Introduction

Lithium ion battery (LIB) technology is quite mature and opted for powering portable devices and electric vehicles. Although LIB plays a vital role in meeting the present day energy requirements in terms of voltage, power and energy density, the limited resources of lithium remains as a question which indirectly puts constraints on the economical issues.[1] Sodium possesses similar electrochemical properties and electrode potential (0.3 V above that of Li) in addition to its widespread abundance making Na systems strategic in energy storage research. Thus, it could serve as an alternative to Li ion systems.[2]

Lack of high performance electrode materials that are easy to synthesize, structurally stable and exhibiting higher specific capacities with superior capacity retention are the greatest technical hurdles that has to be overcome in Na ion batteries in order to compete with the pioneering LIB technology.[3] Among various cathodes, 2D-layered transition metal oxides have widely been investigated as cathode materials because of their structural aspects and high capacities.[4] Sodium based layered electrode materials can be categorized into O or P type depending on the accommodation of sodium ions at octahedral or prismatic sites, respectively.[5] It has been generalized that the P2 type systems can deliver higher capacity close to theoretical capacity when compared to O3 type systems because of its high structural stability during Na-ion insertion/removal.[6-8]

Among the P2 based systems, $Na_{0.67}MnO_2$ is one of the widely studied cathode materials for sodium ion batteries with a discharge capacity of about >175 mAh/g. However, the presence of high spin Mn^{3+} which is a Jahn-Teller ion, increases the electronic localization

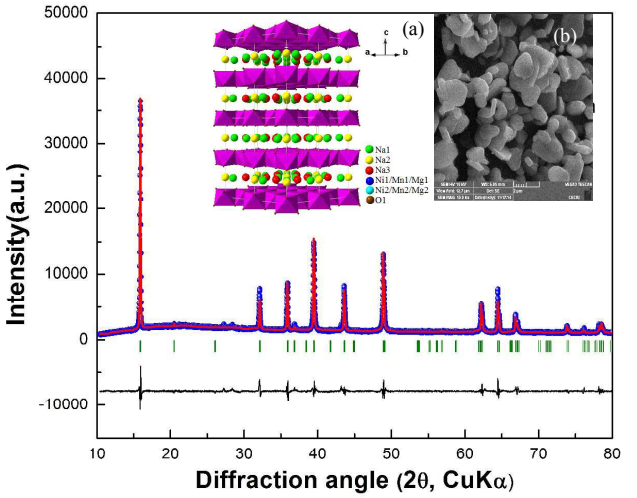

Fig. 1. Structure and Rietveld fit for XRD pattern of P2-$Na_{0.67}Ni_{0.25}Mg_{0.1}Mn_{0.65}O_2$. Insets: (a) Structure of P2 phase showing sodium in three coordinations: Na(1) in green color, Na(2) in yellow color and Na(3) in red color, and (b) SEM image of P2-$Na_{0.67}Ni_{0.25}Mg_{0.1}Mn_{0.65}O_2$

[a] CSIR-Central Electrochemical Research Institute-Chennai unit, CSIR Madras Complex, Taramani, Chennai 600113, India
[b] Academy of Scientific and Innovative Research (AcSIR), CSIR- Central Electrochemical Research Institute-Chennai unit, CSIR Madras Complex, Chennai 600113, India
[c] Surface Engineering Division, CSIR-National Aerospace Laboratories, HAL Airport Road, Bangalore 560017, India
* Corresponding Author
‡ Equally contributing first authors

† Electronic supplementary information (ESI) available: Experimental section, XRD with Rietveld fit and refined crystallographic parameters for the charged and discharged samples and cycling performance at 0.1C are available online or from the authors. See DOI: 10.1039/x0xx00000x

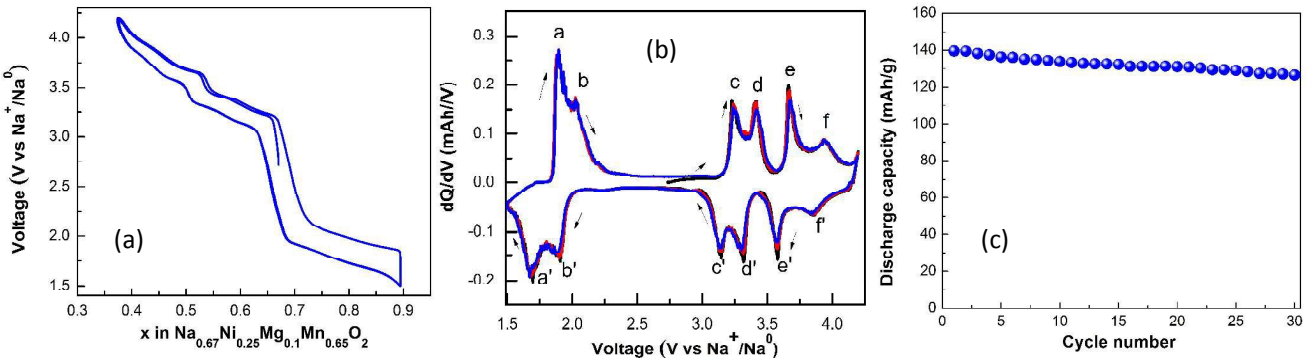

Fig. 2. Electrochemical performance of P2-$Na_{0.67}Ni_{0.25}Mg_{0.1}Mn_{0.65}O_2$ Vs. Na half cells in the voltage range 1.5 - 4.2V at C/10 rate. (a) Voltage vs. composition profile - to show the number of moles of intercalated/deintercalated Na. (b) Derivative plot for the first (black), second (blue) and 3rd (red) cycles, (c) Capacity retention of P2-$Na_{0.67}Ni_{0.25}Mg_{0.1}Mn_{0.65}O_2$ Vs. Na half cells in the voltage range 1.5-4.2V at 0.1C rate

due to strong Na^+/e^- binding and thereby decreases the diffusion coefficient.[7] The structure also exhibits multiple voltage plateaus associated with various phase transitions during sodiation and desodiation.[9-13] The substitution of low valency ions in Na_xMnO_2 is reported to minimize the Jahn-Teller effect by oxidizing Mn^{3+} to Mn^{4+} resulting in highly stable 2D framework structures with smooth charge/discharge profile and fairly good capacity retention.[14] This communication reports dual substitution by lower valent and electrochemically active, inactive elements, Ni^{2+} and Mg^{2+}, respectively in P2 type $Na_{0.67}MnO_2$ and studying its performance as a potential cathode material for Na-ion batteries.

Results and discussion

The structure of P2-Na_xMO_2 is presented in Fig. 1a as inset. It consists of MO_2 slabs made of edge sharing MO_6 octahedra. The sodium ions are sandwiched between these MO_2 slabs so as to occupy trigonal prismatic sites (P) and when the unit cell consists of two distinguishable MO_x layers it is denoted as P2. In these systems, sodium ions occupy two distinct prismatic sites. Sodium has three different coordinations which are marked as Na(1), Na(2) and Na(3). The powder X-ray diffraction pattern of the P2 $Na_{0.67}Ni_{0.25}Mg_{0.1}Mn_{0.65}O_2$ is presented in Fig. 1. All the peaks are indexed to a hexagonal system with space group *$P6_3/mcm$* (Space group No. 193). The refined lattice parameters are *a=b=5.002Å, c=11.1410* Å. The refined crystallographic data of the P2 phase are given in ESI-1. The scanning electron micrograph of P2 phase is presented in Fig. 1b as inset. Polyhedral shaped crystals with the particle sizes ranging from 1 to 2 µm are observed. EDX analysis supported the chemical composition of the compound ($Na_{0.66}Ni_{0.25}Mg_{0.09}Mn_{0.65}O_2$). This is further supported with elemental analysis by AAS.

Galvanostatic charge-discharge experiments were carried out with sodium half cells. The voltage - composition profile for P2-$Na_{0.67}Ni_{0.25}Mg_{0.1}Mn_{0.65}O_2$ at C/10 (Insertion/deinsertion of 1Na per formula unit in 10 h) rate in the voltage range of 1.5-4.2 V is shown in Fig.2a. During 1st cycle nearly 0.52 moles of Na was reversibly intercalated with an average voltage of 3.55 V while retaining the crystal structure in the present voltage region (discussed in later section under *ex-situ* XRD studies).[15,16] The 1st discharge capacity is about 140 mAh/g.

As observed in dQ/dV plot (Fig. 2b), all peaks are inherently coupled i.e. each oxidation peak has exact reduction peak with

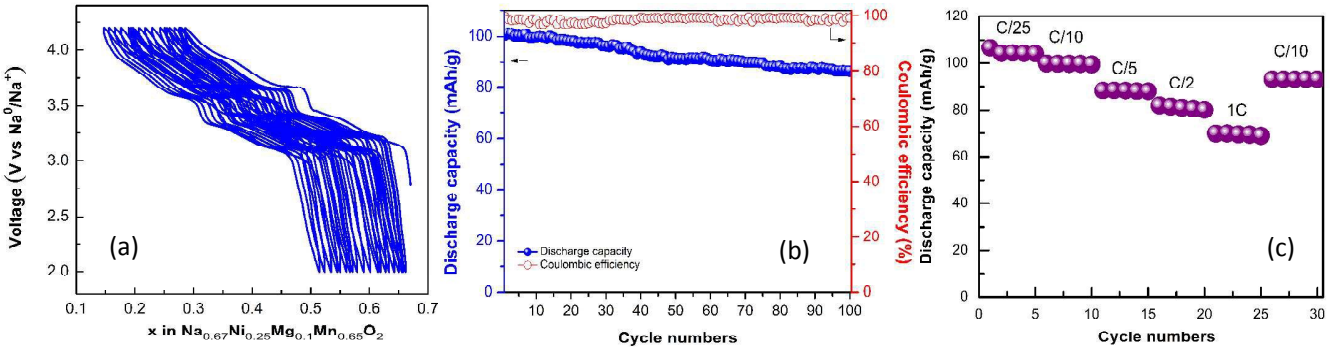

Fig. 3. (a) Cycling profile and (b) Capacity retention plot of $Na_{0.67}Ni_{0.25}Mg_{0.1}Mn_{0.65}O_2$ in the voltage range 2.0 – 4.2V at 0.1C rate, (c) rate performance of P2-$Na_{0.67}Ni_{0.25}Mg_{0.1}Mn_{0.65}O_2$ was tested at different current densities in the voltage range 2.0-4.2 V.

nearly same peak current and similar peak separation between each couple. In other words, each redox/phase transition corresponding to a peak is expected to be electrochemically reversible. Two prominent peaks associated with redox couples (E_{ox}/E_{red}) at 1.89 V/1.68 V (a/a') and 2.02 V/ 1.9 V (b/b') are observed below 3V. There are three strong peaks associated with redox couples (E_{ox}/E_{red}) at 3.22 V/3.14 V (c/c'), 3.39 V/ 3.32 V(d/d') and 3.65 V/3.57 V (e,e') and a weak broader peak is observed at 3.92 V/3.87 V (f/f') above 3 V. In subsequent cycles, the oxidation and reduction peaks show slender shift of ~0.02 V towards positive and negative potentials, respectively. As reported by Dahn *et. al*, the peaks below 3.8 V were due to single phase intercalation or continuous phase transitions. Above 4.2 V two phases (O2+P2) coexisted and at 4.4 V only O2 phase with stacking faults was observed.[15] The charging cut-off potential was restricted to 4.2 V to eliminate the irreversible loss due to phase transformation from P2 to O2 occurring at potentials above 4.2 V. Lee *et al.* indicated the transformation of P2 to O2 at 4.22 V in $Na_{0.67}Ni_{0.33}Mn_{0.67}O_2$ using first principle calculation of formation energy and confirmed by *ex-situ* synchrotron XRD.[17] $Na_{0.67}Ni_{0.25}Mg_{0.1}Mn_{0.65}O_2$ retained 89% of its initial capacity after 30 cycles at C/10 rate in the voltage range 1.5-4.2 V (Fig. 2(c)).

Considering the practical aspects of employing $Na_{0.67}Ni_{0.25}Mg_{0.1}Mn_{0.65}O_2$ as cathode for sodium ion batteries, long cycling and rate performance was carried in the voltage range of 2.0-4.2 V. As seen from Fig. 3(a), the cycling profile is smooth unlike the parent P2-$Na_{0.67}MnO_2$ which depicts multiple potential plateaus associated with various phase transformations during sodiation/desodiation.[9] During charging 0.39 moles of sodium was removed and subsequent discharging 0.38 moles of sodium was inserted back into the structure. The corresponding discharge capacity was about 100 mAh/g at C/10 rate with retention of 87% after 100 cycles (Fig. 3(b)). The rate performances of $Na_{0.67}Ni_{0.25}Mg_{0.1}Mn_{0.65}O_2$ are shown in Fig. 3(c). At C/25 rate it exhibits a capacity of about 106 mAh/g which accounts to reversible intercalation of ~0.40 moles of sodium per formula unit. The capacity decreases to 100 mAh/g at C/10 rate. The capacities obtained at C/5, C/2 and 1C rates are 88, 82 and 70 mAh/g, respectively. Significant decrease in capacity beyond C/10 is attributed to limited diffusion of Na-ion at higher rates.

Fig. 4 compares the cycling profiles of $Na_{0.67}Ni_{0.25}Mg_{0.1}Mn_{0.65}O_2$ with $Na_{0.67}MnO_2$ and $Na_{0.67}Ni_{0.33}Mn_{0.67}O_2$ in the voltage range 2 – 4.2 V. It is evident from the figure that substitution of Ni^{2+} and Mg^{2+} in $Na_{0.67}MnO_2$ increases the average potential from 2.59 to 3.35 V. As a result the energy density of $Na_{0.67}Ni_{0.25}Mg_{0.1}Mn_{0.65}O_2$ versus metallic Na anode is calculated to be 335 Wh/kg which is superior to the energy density values of $Na_{0.67}Ni_{0.33}Mn_{0.67}O_2$ (290 Wh/kg) and $Na_{0.67}MnO_2$ (300 Wh/kg) for a cell performing between 2 to 4.2 V. Further $Na_{0.67}MnO_2$ is reported to undergo severe capacity degradation (~50% loss over 100 cycles, details provided in ESI-2]. Partial substitution of Mn with Ni^{2+} and Mg^{2+} in $Na_{0.67}MnO_2$ significantly improves the capacity retention [ESI-2 & 3].

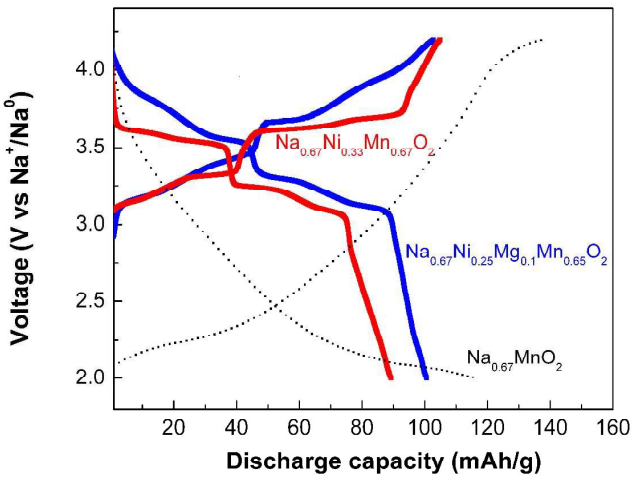

Fig. 4. Cycling profiles of $Na_{0.67}Ni_{0.25}Mg_{0.1}Mn_{0.65}O_2$, $Na_{0.67}Ni_{0.34}Mn_{0.66}O_2$ and $Na_{0.67}MnO_2$ in the voltage range 2- 4.2V at 0.1C rate. For $Na_{0.67}MnO_2$, 1st charge is not shown.

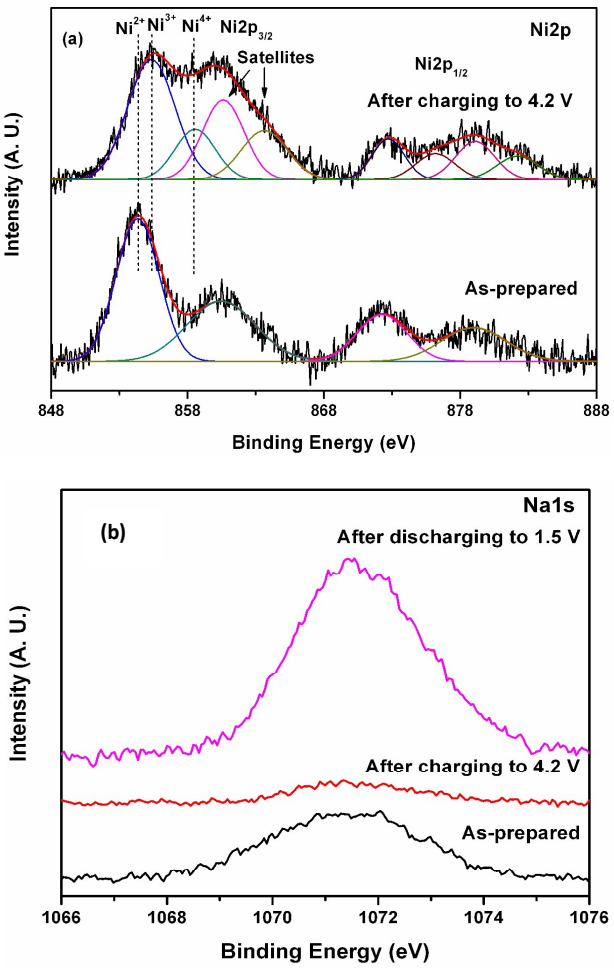

Fig. 5. XPS spectra of as-prepared, charged and discharged samples of P2-$Na_{0.67}Ni_{0.25}Mg_{0.1}Mn_{0.65}O_2$: (a) Ni2p spectra and (b) Na1s spectra.

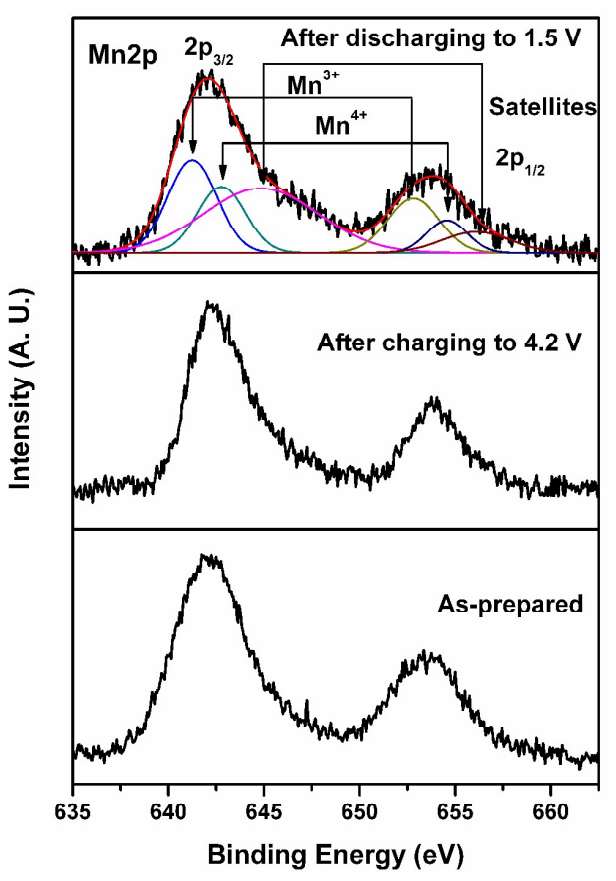

Fig. 6. XPS spectra of as-prepared, charged and dicharged samples of P2-$Na_{0.67}Ni_{0.25}Mg_{0.1}Mn_{0.65}O_2$: Mn2p spectra.

XPS measurements were performed to investigate the oxidation states of Ni, Mn and Na in the pristine and charged samples. In Fig.5, XPS of Ni2p and Na1s core levels in as-prepared P2-$Na_{0.67}Ni_{0.25}Mg_{0.1}Mn_{0.65}O_2$ and the sample after charging to 4.2 V are shown. Ni2p spectral envelopes of as-prepared sample and after charging are observed to be different. In as-prepared sample, $Ni2p_{3/2,1/2}$ peaks at 854.4 and 872.3 eV with spin-orbit separation of 17.9 eV correspond to Ni^{2+}.[18] Broad envelope of Ni2p core level spectrum of the sample after charging to 4.2V indicates that Ni is in multiple oxidation states and it can be curve-fitted into sets of spin-orbit doublets along with associated satellite peaks. Accordingly, sets of $Ni2p_{3/2,1/2}$ peaks at 855.6, 872.7 and 858.3, 876.1 eV are assigned to Ni^{3+} and Ni^{4+} species, respectively.[19,20] Relative intensities of Ni^{3+} and Ni^{4+} are 70% and 30%, respectively. Observed higher binding energy peaks with respect to main peaks are related to corresponding characteristic satellite peaks of $2p_{3/2}$ and $2p_{1/2}$. The oxidation state of Ni is +2 in pristine sample and combination of +3 and +4 is observed in the charged sample. Na1s peak at 1071.4 eV is attributed to Na^+ species[21]. It is important to note that amount of Na decreases after charging, whereas it increases after discharging as seen in Fig. 5b. XPS of $Mn2p_{3/2,1/2}$ core levels in as-prepared P2-$Na_{0.67}Ni_{0.25}Mg_{0.1}Mn_{0.65}O_2$ and the sample after charging to 4.2 V and discharging to 1.5 V are shown in Fig. 6. $Mn2p_{3/2,1/2}$ core level peaks at 642.2, 653.9 eV in as-prepared sample and after charging are assigned for Mn^{4+} species.[22] However, the sample after discharging to 1.5 V contains both Mn^{3+} and Mn^{4+} peaks at 641.1 and 642.2 eV.[22] Thus, it has been confirmed that the capacity above 2V originates from the contributions of Ni^{2+}/Ni^{4+} redox couple and Mn remains in +4 oxidation state. On the other hand, the capacity below 2V is attributed to Mn^{+4}/Mn^{3+} redox.

Structural rearrangement in P2-$Na_{0.67}Ni_{0.25}Mg_{0.1}Mn_{0.65}O_2$ after charging and discharging was studied by ex situ powder X-ray diffraction. Rietveld fit of the XRD patterns and obtained crystallographic parameters are presented in ESI-4 and ESI-5. The powder XRD patterns were refined using both the hexagonal model system, *P6₃/mcm* and orthorhombic system, *Cmcm* space group. The refinement is best converged with the orthorhombic system for the sample charged up to 4.2 V. Further (102) diffraction peak at 40° for the pristine sample indexed in hexagonal system splits into two peaks at 38.4° (022) and 39.7° (112) reflections of orthorhombic symmetry. Hence, an orthorhombic model system, *Cmcm* (No.63) was used to fit the charged sample and an improved fit was obtained (ESI-4).[23-25] During charging, 'c' parameter is found to increase from a value of 11.1395 Å to 11.3889 Å. The refined structure model indicates that four of the M–O bonds contract and two M–O bonds are found to elongate. XRD pattern of the sample discharged from open circuit voltage to 1.5 V is presented in ESI-5. The discharge pattern is best fitted with *P6₃/mcm* hexagonal model system. The 'c' parameter for discharge sample did not appreciably change compare to the pristine sample and the M-O bond length change is symmetrical along all the axes.

The b/a ratio for the charged samples indexed in *Cmcm* model system deviates from the value of 1.732 of an ideal undistorted hexagonal phase in the orthorhombic cell.[24] Further, the ratio between b/(√3a) is slightly higher than unity indicates the distortion within the *ab* plane.[25] Hence, these observations indicate that P2-$Na_{0.67}Ni_{0.25}Mg_{0.1}Mn_{0.65}O_2$ hexagonal phase undergoes orthorhombic distortion during charging and transform to the original hexagonal structure during discharging.

Conclusions

Layered P2-$Na_{0.67}Ni_{0.25}Mg_{0.1}Mn_{0.65}O_2$ is reported as cathode material for rechargeable Na-ion batteries. It exhibited a specific capacity of 140 mAh/g in the voltage window of 1.5-4.2V. Origin of capacity is attributed to $Ni^{2+}/Ni^{3+}/Ni^{4+}$ and Mn^{3+}/Mn^{4+} redox which are active respectively above and below 2V. P2-$Na_{0.67}Ni_{0.25}Mg_{0.1}Mn_{0.65}O_2$ phase undergoes orthorhombic distortion during charging and retains the hexagonal phase during discharging. Replacing part of Mn with Ni^{2+}/Mg^{2+} in $Ni_{0.67}MnO_2$ enhances the average potential by 760 mV and the resultant energy density is calculated to be 335 Wh/kg which is superior to $Ni_{0.67}MnO_2$ and $Na_{0.67}Ni_{0.33}Mn_{0.67}O_2$. In summary, we conclude that substituting Ni^{2+} and Mg^{2+} ions in $Na_{0.67}MnO_2$ facilitates; smoother cycling profile, improved capacity with better retention, increased average potential, thereby enhanced energy density. We believe the approach and the material proposed pave way forward to realize low cost rechargeable Na-ion batteries.

Acknowledgements

Ms. K. Hemalatha and Dr. M. Jayakumar thank Council of Scientific and Industrial Research (CSIR) for granting Senior Research Fellowship and CSIR-Nehru Postdoctoral Fellowship, respectively.

Notes

† The authors claim no competing financial interest

References

1 http://en.wikipedia.org/wiki/Abundance of the chemical elements; R. S. Carmichael, Practical Handbook of physical properties of Rocks and Minerals; CRC Press: Boca Raton, FL 1989; David. R. Lide, Handbook of Chemistry and Physics, Special student Edition, CRC Press, 77th edition, 1996.
2 B.L. Ellis and L.F. Nazar, *Curr. Opin. Solid State Mater. Sci*, 2012, **16**, 168-177.
3 M. D. Slater, D. Kim, E. Lee and C. S. Johnson, *Adv. Funct. Mater.*, 2013, **23**, 947-958.
4 V. Palomares, M. C. Cabanas, E. C. Martinez, M. H. Han and T. Rojo, *Energy Environ. Sci.*, 2013, **6**, 2312-2337.
5 C. Delmas, C. Fouassier, P. Hagenmuller, *Physica B*, 1980, **99**, 81-85.
6 K. Kubota, N. Yabuuchi, H. Yoshida, M. Dahbi and S. Komaba, *MRS Bulletin*, 2014, **39**, 416-422.
7 A. Mendibourne, C. Delmas and P. Hagenmuller, *Journal of Solid State Chem.*, 1985, **57**, 323-331.
8 I. Saadoune, A. Maazaz, M. Menetrier, and C. Delmas, *J. of Solid State Chem.*, 1996, **122**, 111-117.
9 A. Caballero, L. Hernan, J. Morales, L. Sanchez, J. Santos Pena and M. A. G. Aranda, *J. Mater. Chem. A*, 2002, **12**, 1142-1147.
10 D. Su, C. Wang, H.J. Ahn and G. Wang, *Chem. Eur. J.*, 2013, **19**, 10884-10889.
11 N. Yabuuchi, M. Kajiyama, J. Iwatate, H. Nishikawa, S. Hitomi, R. Okuyama, R. Usui, Y. Yamada and S. Komaba, *Nature Materials*, 2012, 11, 512-517.
12 X. F. Wang, M. Tamaru, M. Okubo and A. Yamada, *J.Phys. Chem. C*, 2013, **117**, 15545-15551.
13 D. Yuan, W. He, F. Pei, F. Wu, Y. Wu, J.F. Qian, Y.L. Cao and H. Yang, *J. Mater. Chem. A*, 2013, **1**, 3895-3899.
14 M. H. Han, E. Gonzalo, G. Singh and T. Rojo, *Energy Environ. Sci.*, 2015, **8**, 81-102.
15 Z. Lu and J. R. Dahn, *J. Electrochem. Soc.*, 2001, **148**, A1225-A1229.
16 H. Wang, B. Yang, X.-Z. Liao, J. Xu, D. Yang, Y.-S. He, Z.-F. Ma, *Electrochim. Acta*, 2013, **113**, 200-204.
17 D. H. Lee, J. Xu and Y. S. Meng, PCCP, 2013, **15**, 3304-3312
18 C.L. Aravinda, P. Bera, V. Jayaram, A.K. Sharma and S.M. Mayanna, *Mater. Res. Bull.*, 2002, **37**, 397-405.
19 K.M. Shaju, K.V. Ramanujachary, S.E. Lofland, G.V.S. Rao and B.V.R. Chowdari, *J. Mater. Chem.*, 2003, **13**, 2633-2640.
20 A.I. Inamdar, A.C. Sonavane, S.M. Pawar, Y.S. Kim, J.H. Kim, P.S. Patil, W. Jung, H. Ima, D.-Y. Kim and H. Kim, *Appl. Surf. Sci.*, 2011, **257**, 9606-9611.
21 A. Mekki, D. Holland, C.F. McConville and M. Salim, *J. Non-Cryst. Solids*, 1996, **208**, 267-276.
22 W. Tan, Q. Zhong, D. Xu, H. Yan and X. Zhu, *Int. J. Hydrogen Energy*, 2013, **38**, 16656-16664
23 J-P. Parent, R. Olazcuaga, M. Devalatte, C. Fouassier, P. Hagenmuller, *J. Solid Stat Chem*., 1971, **3**, 1-11.
24 B. M. de Boisse, D. Carlier, M. Guignard, L. Bourgeois and C. Delmas, *Inorg. Chem.* 2014, **53**, 11197−11205.
25 T. Zhou, D. Zhang, T. W. Button, A. J. Wright and C. Greaves, *J. Mater. Chem.,* 2009, **19**, 1123–1128.
26 M. Sathiya, K. Hemalatha, K. Ramesha, J.M. Tarascon and A.S. Prakash, *Chem. Mater.*, 2012, **24**, 1846-1853.
27 H.M. Rietveld, *J. Appl. Crystallogr.*, 1969, **2**, 65-71.
28 J. Rodriguez Carvajal, *Physica B*, 1993, **192**, 55-69.
29 G. Liu, L. Wen, Y. Li, Y. Kou, *Ionics* 21, 2015, 1011-1016
30 W. Zhao, H. Kirie, A. Tanaka, M. Unno, S. Yamamoto, H. Noguchi, *Mater. Lett.*, 2014, **135**, 131-134
31 H. Yoshida, N. Yabuuchi, K. Kubota, I. Ikeuchi, A. Garsuch, M. Schulz-Dobrick and S. Komaba, *Chem. Commun.*, 2014, **50**, 3677-80
32 H. Wang, B. Yang, X.-Z. Liao, J. Xu, D. Yang, Y-S. He, Z-F. Ma, *Electrochim. Acta,* 2013, **113**, 200-204
33 D. Yang, X-Z. Liao, J. Shen, Y-S. He, Z-F. Ma, *J. Mater. Chem. A* 2014, **2**, 6723-6726
34 N. Bucher, S. Hartung, A. Nagasubramaniam, Y.L. Cheah, H.E Hoster, S. Madhavi, Appl. Mater & interfaces. 2014, **6**, 8059-8065
35 D. Su, C. Wang, H.J. Ahn, G. Wang, Chem. Eur. J. 2013, **19**, 10884-10889

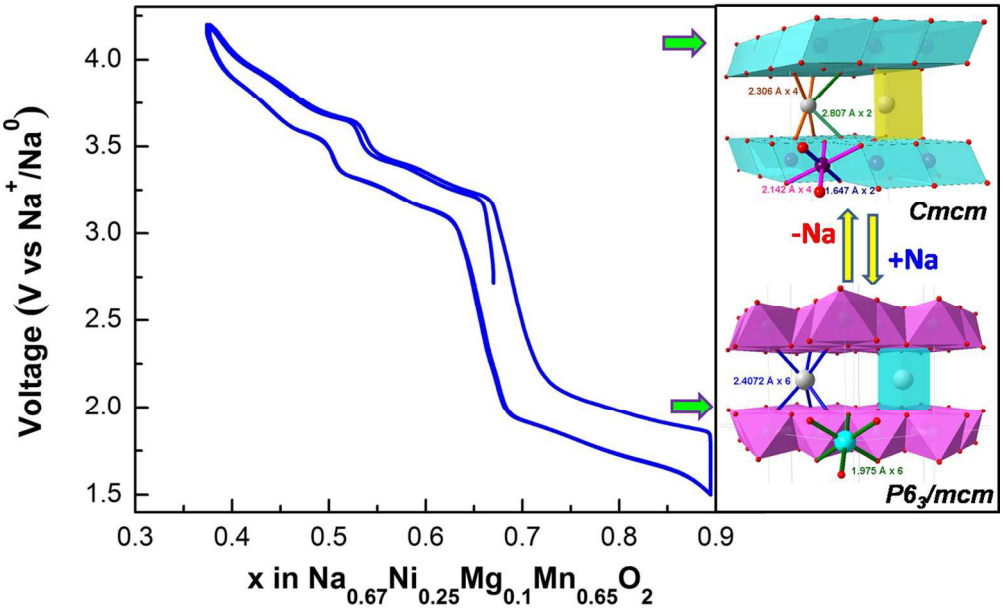

Improved electrochemical performance of Na0.67MnO2 through Ni and Mg substitution
251x156mm (150 x 150 DPI)